Key Parameters in Hollow Embossing Rolling of Metallic Bipolar Plates

Sebastian Heidrich[1] , Martin Wagner[1], Robin Kurth[1], Franz Reuther[1], Steffen Ihlenfeldt[1,2]

[1]Fraunhofer Institute for Machine Tools and Forming Technology
Reichenhainer Straße 88, Saxony, Germany, 09126 Chemnitz
Phone: +49 371 53971721
Email: sebastian.heidrich@iwu.fraunhofer.de

[2]Chair of Machine Tools Development and Adaptive Controls,
TUD Dresden University of Technology
Helmholtzstraße 10, Saxony, Germany, 01069 Dresden
Phone: +49 351 463-34358
Email: steffen.ihlenfeldt@tu-dresden.de

ABSTRACT

Hollow embossing rolling (HER) is an innovative process in which two oppositely embossed rollers continuously form strip metal into a variety of complex three-dimensional shaped goods. This new rolling technology enables the time- and cost-enhanced manufacture of bipolar half-plates for fuel cells and electrolyzers, and it can potentially be used for producing components of HVAC appliances or of consumer electronic devices. While first, predominantly simulation-based, improvements of HER have been achieved, it lacks an experimental investigation of the process's key parameters. Here, these key parameters are identified, and the importance of the interaction effects in HER is shown.

Keywords: Hollow Embossing Rolling, Roll Forming, Rolling, Bipolar Plate, Fuel Cell

INTRODUCTION

Rolling industry has traditionally thrived for optimizing costs and energy usage as well as the quality of produced goods while keep using a long-established process [1]. Today, a variety of different shapes and materials can be manufactured by rolling, including billets, blooms, plates, and ingots on the input and slabs, cross-sections, and plates etc. on the output side [2]. The recent process of Hollow Embossing Rolling (HER) expands this portfolio of rollable goods. It uses oppositely arranged rotating forming rollers (a punch and a die) to continuously form channel geometries into metal sheet strip material [3]. Research on HER ([3–11]) has mainly focused on bipolar plates (BPPs). BPPs serve as media distributors in electrolyzers and fuel cell stacks [10] such as the mobility's sector proton-exchange membrane fuel cell (PEMFC) [12]. They are typically composed of an anode and a cathode [13]; both of them are referred to as bipolar half plates (BPHPs) [4]. There is a definite need for the competitiveness of PEMFCs for BPPs to become less pricey in production and mass-manufacturable (~ 350 to 500 BPPs/fuel stack [4, 14]), which is possible by introducing new manufacturing processes that account for these demands [14].

While metallic, graphite, and polymer-carbon composite BPPs are spread [15], this paper exclusively focuses on the first mentioned category. Metallic BPPs are associated with enhanced physical, mechanical, and chemical properties [16], durability, a less expensive manufacturing, and lower material costs [17]. To evaluate today's manufacturing processes and technology concepts for the production of metallic BPPs, first, a concise comparison of these processes is presented. Emerging from the shortcomings of these technologies, prior processes to HER are introduced. The adjacent chapter gives an overview on HER-related research for BPPs and the key parameters considered in research. With the existing machinery at Fraunhofer IWU, parameter studies were conducted to enrich the research on HER. The results of these experiments are presented in detail. Finally, the technical paper closes by indicating future research required in the field of HER.

CONVENTIONAL AND CONCEPTIONAL PROCESSES FOR METALLIC BPPS

The manufacture of metallic BPPs typically follows a defined sequence that is denoted by [18] as "forming, separating, joining". After forming the flow field geometry into the metal sheet, the anode and cathode BPHP are trimmed, and finally these sides are joined together to form a functional BPP [18]. Regarding the first step of creating the BPP geometry by forming, a variety of established and conceptionally modeled processes have been investigated. In the following, a selection of these processes shall be presented.

In hollow embossing, a metallic sheet is formed using high pressing forces applied by two rigid counter dies, in which the material lies [13, 19]. Stamping, in general, is renowned for its productivity, high volume capabilities, and cost-efficiency [17, 20]. However, it exhibits technological issues in terms of the forming limit [20] and idle time due to its discontinuous nature. Another forming technology investigated for metallic BPP is rubber pad forming [15]. It uses a rigid die and an elastic rubber pad die for the application of counter-pressure as tooling [15]. The reduction to one rigid die and the usage of a soft counter die ease the tooling production and assembly process, leading to cost-efficiency and time savings [21]. However, the geometrical accuracy of the workpiece is not ensured because of the rubber pad die [21, 22], which has a short lifespan [15]. In hydroforming, a pressurized liquid media operating in the cavity between a set of dies forms the geometry of a clamped sheet via hydropressure [21]. Here, the well-known forming limit issue needs to be solved [20], and a currently low productivity [18] worsen the process's performance. Regarding micro-processes such as micro-electrical-discharge machining (micro-EDM), micro-stamping, micro-electromagnetic forming, incremental micro-forming, and micro-roll forming have also been investigated in the context of metallic BPPs [6, 13, 14, 21–23]. Latter shall be reviewed together with other roll forming technologies to be compared to HER. While micro-EDM suffers from low attractiveness in terms of quality and production-/cost-efficiency [22], the economically efficient process of micro-stamping is constrained by technological limitations regarding the material thinning and channel formation [21, 23]. Incremental micro-forming is currently not suited for application in high volume industrial production , though it shows potential for usage in early research stages of BPHPs [13]. Micro-electromagnetic forming excels traditional stamping in terms of its tooling cost-advantages and simplicity [14]. However, technological challenges, such as the conductivity properties of the BPP material or the pressure distribution needed for their manufacturing, prevail [14]. Overall, the mass-scale production of BPPs by micro-manufacturing technologies is adversely affected by the tribological conditions and service life issues of the utilized tooling [16].

Comparing the mentioned processes for metallic BPPs, hollow embossing and hydroforming are industrially established while providing a qualitative way of manufacturing BPPs. However, the achievable production rates are limited due to the nature of these processes. Therefore, in recent years, the continuous forming of BPPs by rolling has gained momentum. With HER, the manufacturing of metallic BPPs in a high speed manner, i.e. up to 120 BPHP/min, is envisioned [13, 24].

HOLLOW EMBOSSING ROLLING AND SIMILAR PROCESSES

Technological Pre-Developments Enabling Hollow Embossing Rolling

The basic idea behind HER to form the shape of a metallic strip sheet by means of a set of embossing rollers, is not entirely new. For example, [25] describe an embossing machine and the manufacturing of its embossing rollers. Moreover, [26] filed a patent for a pair of embossing jackets for rotary register embossing rollers used for the process's sheet metal forming. [27] exhaustively describes the usage of a sub-licensed process consisting of oppositely engraved interlocking rollers for the manufacture of spherically embossed strip goods by bending and stretching deformation at Dunford Hadfields Ltd. in Sheffield, 1969. Similarly to HER, one roller's vertical position can be adjusted to apply a defined force against the other roller [27]. However, the manufactured workpieces differ much from today's thin foil BPPs. [27] lists the utilized machinery (five to 250 ton compressive capacity) and strip specifications (0.635 mm to 2.032 mm max. thickness, 304.8 mm to 1,676.4 mm width).

Contrarily, BPPs in research on HER and/or similar processes typically have a thickness ranging from 0.05 mm to 0.1 mm and consist of metal strips such as stainless steel [3, 4, 6, 7, 10, 19, 23]. Regarding the sub-millimeter scale of the channel geometries in BPPs [7, 11], recent research activities have greatly expanded the applications of the underlying forming principle. In the past years, multiple research works have been published that explicitly aim to manufacture BPHP-typical channel geometries by rolling technology. Due to the process' principles, however, only continuous longitudinal or transversal channel geometries were produced with these preliminary forming processes (further referred to as similar processes are [23, 28–30]). These studies provided the basis for development of HER, which was first introduced by Bauer et al. [4] as "roll forming". To better account for this researched process's similarity to the well-established hollow embossing, Reuther et al.Klicken oder tippen Sie hier, um Text einzugeben. [7] adopts the term "hollow embossing rolling" (HER). Latter term has spread across the field and is also used by this paper as it follows this convention.

Research on Hollow Embossing Rolling

As described above, the continuous forming of channel geometries in HER is realized by a synchronous roller rotation of a punch and a die roll. Since these rollers contain an arbitrarily complex, discontinuous engraving, the restrictions of legacy

and/or similar processes no longer arise. In the publications of Bauer [5] and Bauer et al. [4], both experimental and numerical studies were conducted to demonstrate the overall prowess of the process principle and to increase the HER-related understanding. Quality-relevant criteria of BPHPs, such as wrinkling and flatness deviations, were evaluated and optimization potentials were described, primarily on the basis of forming simulations. Initial technological key parameters such as the rolling gap and the strip tension were presented and partially evaluated on the basis of numerical studies, although a well-founded experimental study was not possible due to the used machine technology. The studies published by Reuther et al. [7, 10, 11, 31–33] in particular further developed the numerical modeling and its accuracy. Initial experimental studies on discontinuous BPHP test geometries confirmed the suitability of HER for BPPs and also demonstrated the influence of the strip tension on wrinkling tendencies and the thinning behavior. More efficient modeling approaches have increased the complexity of the BPHP geometries that were simulated, so that extensive numerical studies on the technologically influencing variables were possible. Based on this work, the key process parameters in machine development can be identified as strip tension and clamping or forming force. Moreover, relevant disturbance variables result from the rollers' elasticity, which contributes to load-dependent rolling gap changes, friction, a misalignment between the rollers, and manufacturing-related inaccuracies of the roller engravings.

Accounting for both types of investigation, numerical and/or experimental, table 1 illustrates the set parameters in HER-related research. While different BPP plate dimensions *PD* (e.g. [3, 5, 11, 31]) and material thickness *t* (e.g. [8, 24, 32]) were employed, variations in the target rolling gap *RG* ([5, 11]) and/or forming force F_z ([3, 9]), the rolling direction *RD* ([4, 5, 11]), the strip tension σ_x ([7, 11]), the rotational speed of the rollers ω ([5, 6, 11]), the roller diameter *d* ([5, 6, 11]), and the clamping force $F_{z,c}$ ([11]) occurred, there is a lack of consistency in terms of parameter selection and an insufficient experimentally-based clarification regarding the importance of these parameters across the research base. For this reason, it is, that this paper tries to clarify the key parameters in HER. Using one selected BPP design, a defined set of rollers, and the often chosen 1.4404 material, experimental parameter studies were conducted.

Table 1. Parameters as defined in HER-related numerical and experimental studies.

	[4]	**[5]**	**[8]**	**[24]**	**[3]**	**[10]**	**[7]**	**[6]**	**[34]**	**[33]**	**[9]**	**[11]**	**[35]**
Material	1.4404	1.4404	1.4404	1.4404	1.4404	1.4404	1.4404	1.4301	1.4404 TiG1	-	S	1.4404	1.4404
***t* in mm**	0.1	0.1	0.05	0.1	0.1	0.1	0.1	0.1-0.2	0.5	0.1		0.1	0.1
***PD* (mm x mm)**	52 x 28	52 x 28 / 74 x 40	100 x 50	50 x 50	50/210 (wide)	45 x 30	45 x 30	-	300 x 350	45 x 30 / 380 x 150	x	45 x 30 / 70 x 50, 55,60; 380 x 150	150 x 3810
RG* in mm	0.12	0.12, 0.08 - 0.16	-	-	-	0.1	0.1	-	-	0.1	-	0.1, 0.085 - 0.115 / 0.1	0.1
***RD* in deg**	0 and 90	0 and 90	-	-	-	-	-	-	-	-	-	0	-
σ_x in N/mm²	x	x	x	-	-	-	0 – 101	-	-	-	-	0 - 101 / 0 - 360, 100 – 150	150
ω in rev./min	3.1	3.1, 12.1 - 28.1	60	20	-	20	20	573 - 1,432.4	-	-	-	3, 20 - 73 / 9.5, 29.6	29.6
***d* in mm**	105	105 /150	105	200	100	105	105	10-160	-	105	-	105, 200 / 100 - 400, 245	245

F_z in kN**	-	-	-	-	25 and 125	-	-	-	-	-	0 - 25	-	-
$F_{z,c}$ in kN	-	-	-	-	-	-	x	-	-	x	-	0,7 - 3 / up to 8.5, 22.5	22.5
*assuming no load-induced deviations	**only considered if varied as input variable						S means steel						

EXPERIMENTAL PARAMETER STUDIES

Machinery at Fraunhofer IWU

Building upon [3, 9], the HER machine configuration at Fraunhofer IWU incorporates three consecutive steps for the metal strip to pass through: the feeding, forming, and an optional guiding stage. On the inlet side, the required strip tension σ_x is induced by means of an adjustable braking torque T_b, which prevents excessive wrinkling from propagating across the rolling direction. In the forming stage, a positive (the punch) and a negative (the die) roller are arranged. This kind of hollow embossing, which is enabled by the synchronized rotation of the tooling, continuously forms the three-dimensional workpiece geometry. After the metal strip passed through the forming stage, a possible third guiding-related stage can be included in the machine setup. For the parameter studies presented within this publication, it was restrained from using the third stage. Figure 1 shows the entire machinery setup with special focus on the forming stage.

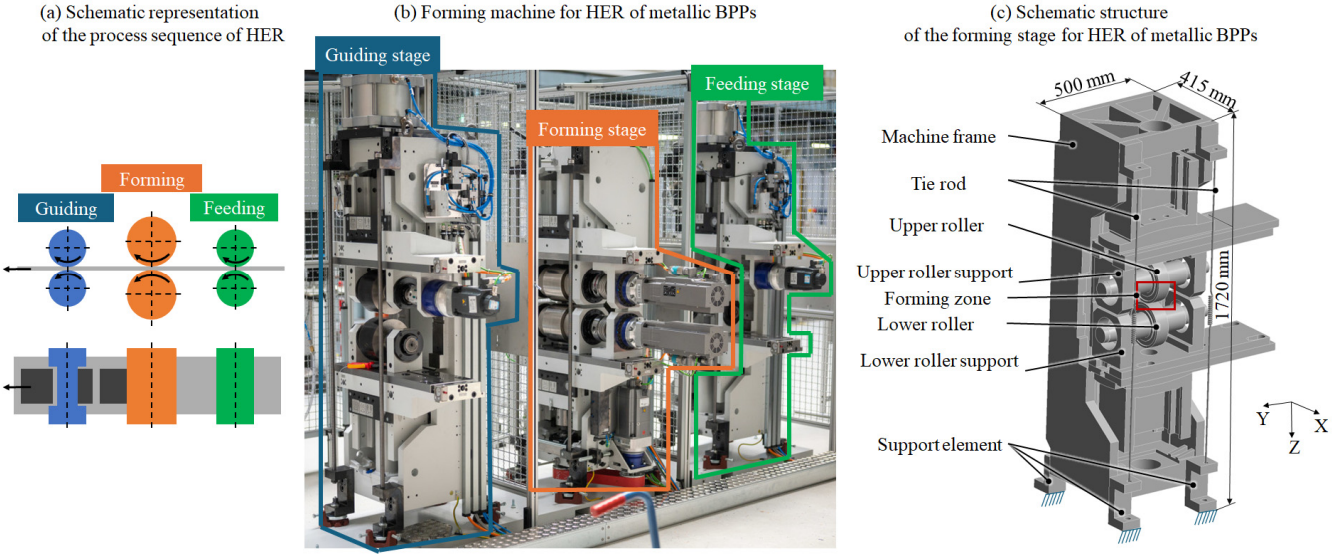

Figure 1. Schematic representation of HER (a), structure of the HER machinery setup at Fraunhofer IWU (b), and schematic CAD-model of the forming stage (c).

Selection of Parameters for HER Experiments

With the constraints imposed by an efficient setup, the roller diameter (d = 243.5 mm) and PD (380 mm x 150 mm per BPHP) (see figure 2) remained the same throughout the experiments. As can be seen by table 1, the selected t = 0.075 mm thick 1.4404 stainless steel lies in-between the typical 0.05 and 0.1 mm thickness for this material grade, which supports a parameter study with fairly balanced results. Given these restrictions, the parameters to be investigated are the strip tension σ_x, the rotational speed ω of the rollers, and the forming force F_z (that already incorporates the clamping force $F_{z,c}$). The influence of RD was not investigated; [4], [5], and [11] showed that the rolling direction's influence is negligible. All of the investigated parameters can either be directly or indirectly adjusted by the machine control.

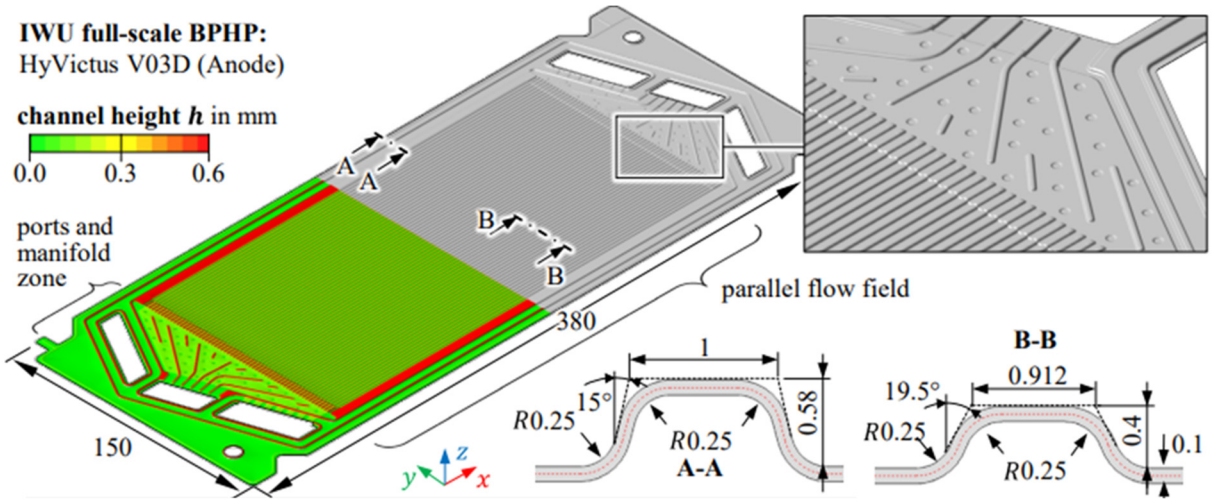

Figure 2. BPP plate geometry shown for the anode BPHP. [33]

Experimental Design

Five different initial strip tensions σ_x were applied as a restraining tension on the inlet side (B2 to B5), four experiments investigated the variation of the initial forming force (C1 to C4), and another four experiments focused on speed variations (D1 to D4) (see table 2). In the following analysis, experiment B1 serves as a reference (short R). The results for the torque T and the forming force F_z are reported from the perspective of the bottom forming roller for the sake of simplicity.

Table 2. Parameter studies for strip tension (B), rotational speed (C), and forming force (D).

	B1 (R)	**B2**	**B3**	**B4**	**B5**	**C1**	**C2**	**C3**	**C4**	**D1**	**D2**	**D3**	**D4**
σ_x at 0° in N/mm²	85.7	47.3	63.6	104.7	121.4	86.2	84.2	85.3	88.3	88.4	90.5	88.5	93.6
F_z at 0° in kN	28	28.2	28	28.2	28	12.3	19.7	30.7	36.6	26.8	27.8	27.2	27.4
ω in rev./min	12.3	12.3	12.3	12.3	12.3	12.3	12.3	12.3	12.3	24.6	37	49.3	147.8

Experimental Parameter Study Results

As can be seen in figure 3, the forming force and torque of the bottom forming roller roughly follow the geometry of the BPHPs, especially for the cathode side (DP1 to DP3), the media ports and manifold sections, and the transitional area to the anode side (from DP3). There is a sudden increase in forming force and/or torque on both BPHPs when the media ports and manifold areas have been formed, and the linear flow field section starts. On the cathode side, the forming force and torque remain fairly on the same level while the rollers form the linear flow field. This observation does not seem to apply to the anode side (from DP3 to end), where only the torque reaches a plateau for the linear flow field, while the forming force is constantly reduced. Similarly to the increased forming force and torque on the cathode side when entering the linear flow field, the torque and forming force on the anode side sharply decline when leaving the linear flow field area.

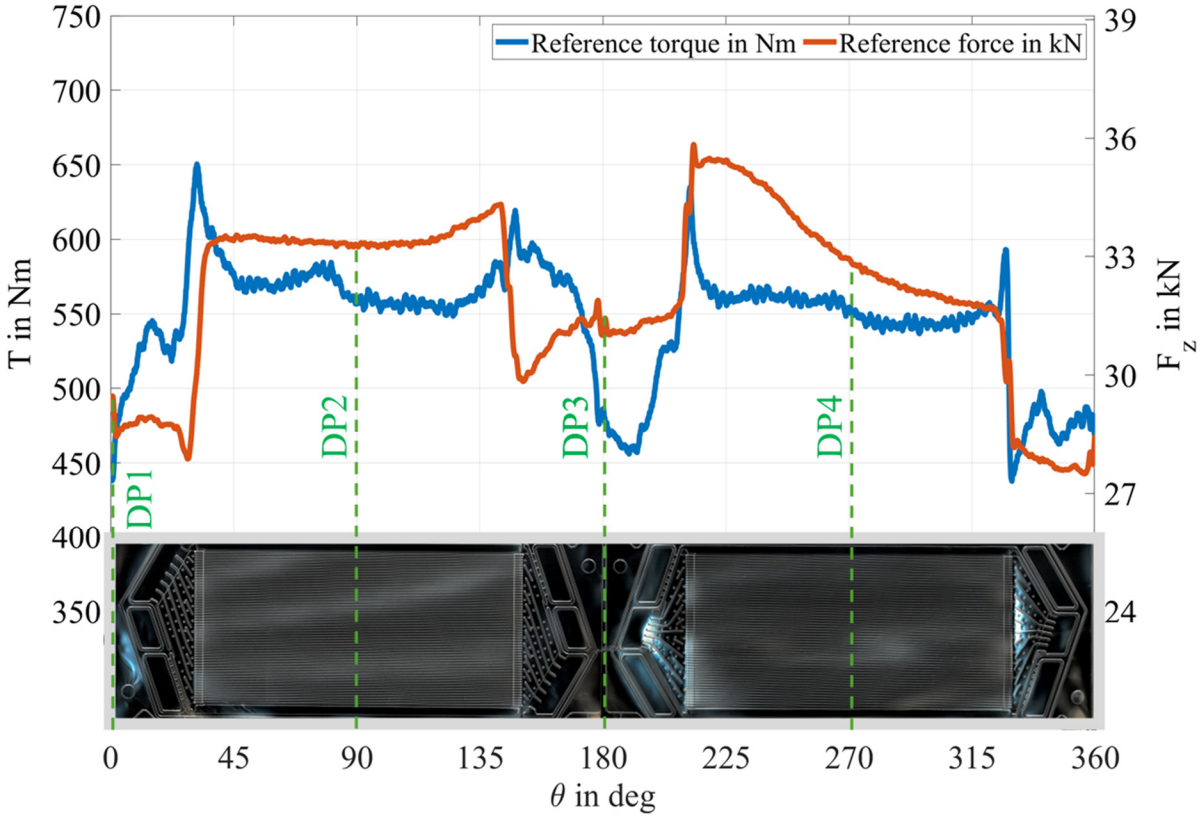

Figure 3. Torque and forming force for the reference experiment. The cathode (from 0-180°) and the anode (from 180-360°) are shown beneath the diagram. The dashed lines represent discrete points (DP1 to DP4) chosen for the correlation analysis.

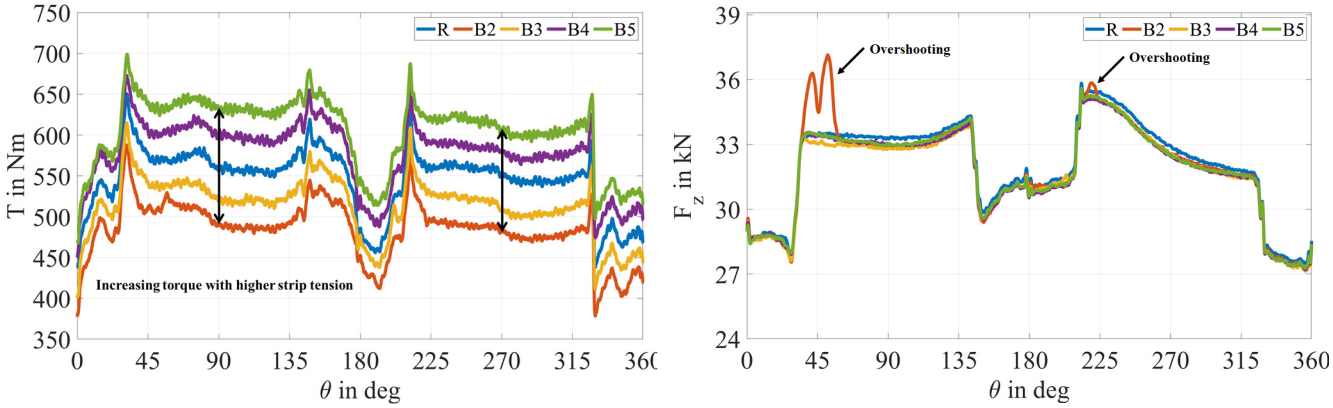

Figure 4. Torque and forming force progression under different strip tensions.

Under variation of the initial strip tension (see figure 4), the torque of the bottom forming roller shows a qualitatively similar progression with a leveled behavior according to the applied restraining tension (from the lowest to the highest strip tension the torque is constantly on a higher level). In contrast to these findings, the forming force does not show this dependency. However, the forming force for B2 shows a high peak value in the beginning areas of the cathode and anode linear flow field. These data points exhibit overshooting issues. A possible explanation for this may be the absence of a sufficient strip tension.

Investigating the variation of the forming force (see figure 5), there are some peculiarities in the bottom roller's torque progression graph. Logically, with an increase in forming force as adjusted, a higher torque is required for forming the BPHPs' geometry. In the anode linear flow field a phenomenon occurs that requires further investigation. For the reference, C3, and C4 data sets there is a rising or constant level of torque at the linear flow field, while C1 and C2 show a declining behavior. At the cathode side (see DP1 to DP3 for reference), only C4, which has the highest pre-set forming force, does not face a sharp decline in torque after the manifold areas have been formed. Moreover, a smaller spread between the data sets is noticeable at the

cathode and anode side exit area. Further investigations regarding the interaction effects in the rolling gap may reveal the underlying reasons for the described deviating torque progression and altered spread between the data sets.

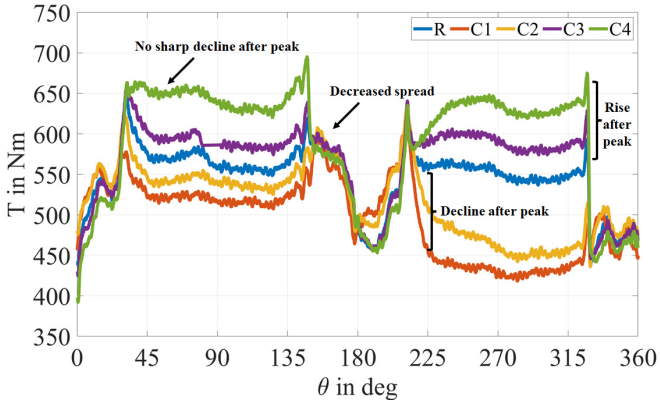

Figure 5. Torque progression under different forming forces.

When increasing the rotational speed of the forming rollers, there is an increased blurriness of the characteristic bottom forming torque and forming force curve with a rise in forming speed and a shift of the linear flow field areas' entry and/or exit is visible. The reference data set (25 mm/s) and the data set D4 (300 mm/s) (see figure 6) depict the highest contrast. Possible reasons for the mentioned blurriness include, but are not limited to, the signaling rate, the elasticities of the rollers, the intricate geometrical design of the rollers, which may possibly lead to inherent manufacturing inaccuracies, and the rollers' inertness.

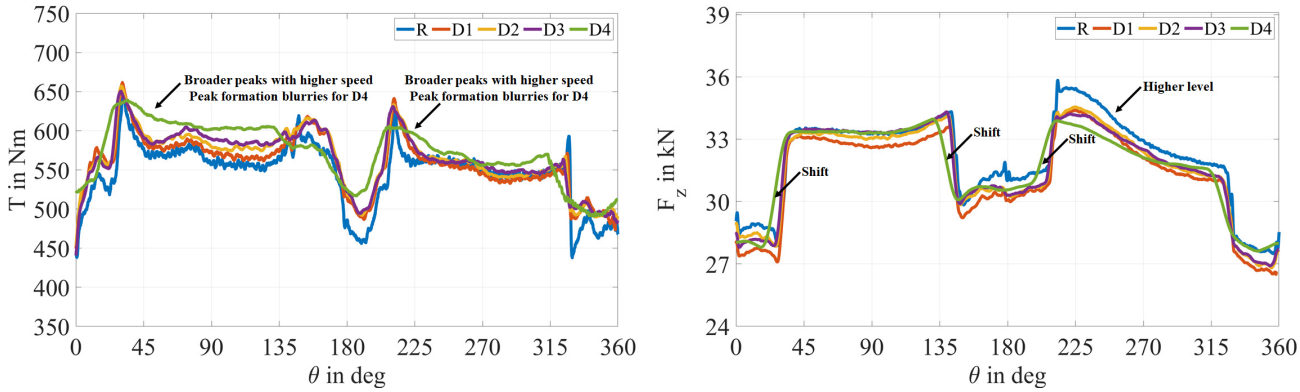

For the interpretation of the experimental results, the interaction effects play a key role as interdependencies between variables shape the HER process. For example, an increase in the bottom forming roller torque leads to a higher strip tension. Therefore, a correlation analysis for the braking torque/strip tension, the roller speed, the torque of the bottom roller, and the forming force was conducted at four discrete data points (DP1 to DP4, see figure 3 for reference). The correlation coefficients gathered in table 3 depict the correlation coefficients as calculated over all reported parameter studies (B1 to D4). While a correlation coefficient of -0.35 to 0.35 is classified as a weak correlation between variables and a correlation coefficient of -0.36 to 0.67/0.36 to 0.67 is considered to indicate a moderate correlations, a correlation coefficient of 0.68 to 1.0 represents a strong correlation [34].

The correlation between the torque of the bottom forming roller T and the rotational roller speed ω as well as the forming force F_Z and the torque of the bottom roller T varies significantly between DP1 to DP4, indicating a geometry and/or material-dependent behavior. Concerning the remaining correlations, there is no change from a former weak correlation to an increased moderate or strong one. However, these more uniform correlations between the DPs allow to make general assumptions about the influence of changing parameters on the process's output. While an increase in the braking torque T_b directly translates into a higher strip tension σ_x, which is reasoned by the machinery setup, it has close to no influence on the rotational roller speed ω or on the forming force F_Z. Latter also applies to the correlation between the strip tension σ_x and the rotational roller speed ω or the forming force F_Z, while the strip tension σ_x shares a moderate to high positive correlation with the torque of the bottom forming roller T. Finally, the forming force F_Z and the rotational roller speed ω show a weak correlation, i.e. a change in one of the both variables does not significantly alter the value of the other one.

Table 3. Correlation coefficients for DP1 to DP4.

	T_b	σ_x	ω	T	F_z
T_b					
DP1	1				
DP2	1				
DP3	1				
DP4	1				
σ_x					
DP1	0.99	1			
DP2	0.99	1			
DP3	1	1			
DP4	0.99	1			
ω					
DP1	0.01	0.14	1		
DP2	0.01	0.09	1		
DP3	0.01	0.09	1		
DP4	0.01	0.12	1		
T					
DP1	0.67	0.72	0.54	1	
DP2	0.74	0.76	0.28	1	
DP3	0.52	0.58	0.76	1	
DP4	0.47	0.49	0.17	1	
F_z					
DP1	-0.01	0.02	0.05	-0.32	1
DP2	0.01	0.00	0.09	0.59	1
DP3	-0.007	-0.02	0.075	0.18	1
DP4	-0.003	0.004	0.038	0.87	1

CONCLUSIONS

This paper has presented research on HER and/or similar processes with a special focus on the key parameters influencing the forming of metallic BPPs. First, after comparing established manufacturing processes for metallic BPPs and showing the path towards development of HER, it discussed the key parameters in HER. While past research further qualified the HER process for industrial usage, there was a lack of systematically and experimentally conducted parameter variation studies on full-scale BPPs that are required for estimating the influence of changing (input) variables on the process and/or on the machinery. Here, the predominantly numerically based research base could be expanded by such experimental investigations. Therefore, three

sets of experiments that sequentially varied the strip tension, the forming force, and the rotational speed of the utilized rollers were conducted and presented.

As a result of these parameter studies, it was revealed that there exist different correlations between the selected parameters in HER, which shape the overall process's output. HER is a complex, multi-variate forming process that is influenced by not only, but also, the specified process parameters, the machinery setup, and/or the current BPP geometry/material. To properly account for the significance of the revealed interaction effects in HER, further investigations based on a larger numbers of experiments and parameter sets are required. Therefore, the authors plan to conduct more elaborate parameter studies and to develop a model for anticipating the parameters' values in HER on basis of these investigations.

ACKNOWLEDGEMENTS

The authors would like to express their sincere gratitude for the financial support received by the "H2GO – National fuel-cell production action plan" project which is funded by the Federal Ministry for Digital and Transport (BMDV) as part of the National Innovation Program Hydrogen and Fuel Cell Technology Phase 2 (NIP II), funding code 03B11027B (funding coordination by NOW GmbH and implementation by project management Jülich), the "HZwo: smartROLL – Sensorintegrierte Anlagenkomponenten zur Überwachung prozessrelevanter Kenngrößen beim Hohlprägewalzen" project, funded by the European Regional Development Fund (ERDF)/tax money from the budget of the Saxonian State Parliament, grant number 100716272, and the task "Development of Manufacturing On-Device AI and Dataspace Technology (ModAI-Platform)" within the project "Joint R&D Project of the Global Industrial Technology Cooperation Center (GITCC)", funded by the Korean Institute for Advancement of Technology, task number P0028468.

REFERENCES

1. B. Buchmayr, M. Degner, and H. Palkowski, "Future Challenges in the Steel Industry and Consequences for Rolling Plant Technologies," BHM Berg- und Hüttenmännische Monatshefte, vol. 163, no. 3, pp. 76–83, 2018, doi: 10.1007/s00501-018-0708-x.
2. S. Y. Jo, S. Hong, H. N. Han, and M.-G. Lee, "Modeling and Simulation of Steel Rolling with Microstructure Evolution: An Overview," steel research international, vol. 94, 2023, doi: 10.1002/srin.202200260.
3. M. Wagner, M. Alaluss, R. Kurth, R. Tehel, F. Reuther, and S. Ihlenfeldt, "Characterization of the Machine Behaviour During Hollow Embossing Rolling of Metallic Bipolar Plates," Journal of Machine Engineering, vol. 23, no. 3, pp. 167–178, 2023, doi: 10.36897/jme/167525.
4. A. Bauer, S. Härtel, and B. Awiszus, "Manufacturing of Metallic Bipolar Plate Channels by Rolling," Journal of Manufacturing and Materials Processing, vol. 3, no. 2, 2019, doi: 10.3390/jmmp3020048.
5. A. Bauer, "Experimentelle und numerische Untersuchungen zur Analyse der umformtechnischen Herstellung metallischer Bipolarplatten," Dissertation, Institut für Werkzeugmaschinen und Produktionsprozesse, Professur Virtuelle Fertigungstechnik, Technische Universität Chemnitz, Chemnitz, 2020. Accessed: Apr. 22 2025. [Online]. Available: https://nbn-resolving.org/urn:nbn:de:bsz:ch1-qucosa2-715389
6. J. Zhang, Z. Chen, H. Zhang, Y. Zeng, and X. Zhang, "Investigation of roll forming process and quality control factors for metal bipolar plates," International Journal of Hydrogen Energy, vol. 93, pp. 898–909, 2024, doi: 10.1016/j.ijhydene.2024.10.433.
7. F. Reuther, M. Dix, V. Kräusel, V. Psyk, and S. Porstmann, "Model validation of hollow embossing rolling for bipolar plate forming," International Journal of Material Forming, vol. 17, 2024, doi: 10.1007/s12289-023-01804-w.
8. M. Fiedler, K. Kittner, and B. Awiszus, "Production of Metallic Bipolar Plates Made of Stainless Steel by Incremental Hollow Embossing Using Rollers," Engineering Proceedings, vol. 26, no. 1, 2022, doi: 10.3390/engproc2022026015.
9. M. Wagner, M. Alaluss, J. Langheinrich, F. Reuther, R. Kurth, and S. Ihlenfeldt, "Prozessüberwachung mittels maschineninhärenter Sensoren," wt Werkstattstechnik online, vol. 114, 01-02, pp. 15–20, 2024, doi: 10.37544/1436–4980–2024–01–02–17.
10. F. Reuther, V. Psyk, V. Kräusel, and M. Dix, Simulation of Hollow Embossing Rolling for Bipolar Plate Forming using LS-DYNA©.
11. F. Reuther, "Simulationsbasierte Prozessauslegung des Hohlprägewalzens zur umformtechnischen Herstellung von Bipolarhalbplatten," Institut für Werkzeugmaschinen und Produktionsprozesse, Technische Universität Chemnitz, Chemnitz, 2025.

12. N. de las Heras, E. P. L. Roberts, R. Langton, and D. R. Hodgson, "A review of metal separator plate materials suitable for automotive PEM fuel cells," Energy & Environmental Science, no. 2, pp. 206–214, 2009, doi: 10.1039/b813231n.

13. S. Porstmann, T. Wannemacher, and W.-G. Drossel, "A comprehensive comparison of state-of-the-art manufacturing methods for fuel cell bipolar plates including anticipated future industry trends," Journal of Manufacturing Processes, vol. 60, pp. 366–383, 2020, doi: 10.1016/j.jmapro.2020.10.041.

14. J. Shang, L. Wilkerson, S. Hatkevich, and G. S. Daehn, "Commercialization of Fuel Cell Bipolar Plate Manufacturing by Electromagnetic Forming," in High Speed Forming 2010 Proceedings of the 4th International Conference, Columbus (Ohio, USA), 2010, pp. 47–56.

15. Y. Liu and L. Hua, "Fabrication of metallic bipolar plate for proton exchange membrane fuel cells by rubber pad forming," Journal of Power Sources, vol. 195, pp. 3529–3535, 2010, doi: 10.1016/j.jpowsour.2009.12.046.

16. M. F. Peker, Ö. N. Cora, and M. Koç, "Investigations on the variation of corrosion and contact resistance characteristics of metallic bipolar plates manufactured under long-run conditions," International Journal of Hydrogen Energy, vol. 36, pp. 15427–15436, 2011, doi: 10.1016/j.ijhydene.2011.08.067.

17. F. Dundar, E. Dur, S. Mahabunphachai, and M. Koç, "Corrosion resistance characteristics of stamped and hydroformed proton exchange membrane fuel cell metallic bipolar plates," Journal of Power Sources, vol. 195, pp. 3546–3552, 2010, doi: 10.1016/j.jpowsour.2009.12.040.

18. S. Porstmann, A. C. Petersen, and T. Wannemacher, "Analysis Of Manufacturing Processes For Metallic And Composite Bipolar Plates," in Konferenzband der ersten FC³ Fuel Cell Conference Chemnitz, Chemnitz, 2019, pp. 25–39.

19. D. Briesenick, M. Beck, K. R. Riedmueller, and M. Liewald, Numerical study on a new forming method for manufacturing large metallic bipolar plates.

20. C. K. Jin and C. G. Kang, "Fabrication process analysis and experimental verification for aluminum bipolar plates in fuel cells by vacuum die-casting," Journal of Power Sources, vol. 196, no. 20, pp. 8241–8249, 2011, doi: 10.1016/j.jpowsour.2011.05.073.

21. L. Peng, P. Yi, and X. Lai, "Design and manufacturing of stainless steel bipolar plates for proton exchange membrane fuel cells," International Journal of Hydrogen Energy, vol. 39, pp. 21127–21153, 2014, doi: 10.1016/j.ijhydene.2014.08.113.

22. H. J. Bong, J. Lee, J.-H. Kim, F. Barlat, and M.-G. Lee, "Two-stage forming approach for manufacturing ferritic stainless steel bipolar plates in PEM fuel cell: Experiments and numerical simulations," International Journal of Hydrogen Energy, vol. 42, pp. 6965–6977, 2017, doi: 10.1016/j.ijhydene.2016.12.094.

23. B. Abeyrathna, P. Zhang, M. P. Pereira, D. Wilkosz, and M. Weiss, "Micro-roll forming of stainless steel bipolar plates for fuel cells," International Journal of Hydrogen Energy, vol. 44, pp. 3861–3875, 2019, doi: 10.1016/j.ijhydene.2018.12.013.

24. S. Porstmann et al., "Zielgrößen und Spannungsfelder beim Vergleich von Herstellungs- verfahren für metallische Bipolarplatten Objectives and fields of tension in the comparison of manufacturing processes for metallic bipolar plates," in FC³ Fuel Cell Conference Chemnitz Saubere Antriebe. Effizient Produziert.: Chemnitzer Brennstoffzellenkonferenz Konferenzband, Chemnitz, 2022, pp. 195–208.

25. F. A. Sunderhauf and J. C. O'Hear, "METHOD OF EMBOSSING ROLLS," US2662002A, Dec 8, 1953.

26. F. W. Broderick, "PROCESS FOR REGISTER EMBOSSING PRINTED SHEET METAL," US3362264A, Jan 9, 1968.

27. Dunford Hadfields Ltd., "Rotary embossing of metals: Engraved fully hardened rolls," METAL FORMING, vol. 36, no. 12, 344-346, 1969.

28. V. V. Nikam and R. G. Reddy, "Corrugated bipolar sheets as fuel distributors in PEMFC," International Journal of Hydrogen Energy, vol. 31, no. 13, pp. 1863–1873, 2006, doi: 10.1016/j.ijhydene.2006.03.004.

29. P. Zhang, M. Pereira, B. Rolfe, W. Daniel, and M. Weiss, "Deformation in Micro Roll Forming of Bipolar Plate," in 36th IDDRG Conference - Materials Modelling and Testing for Sheet Metal Forming 2–6 July 2017, Munich, Germany, Munich (Germany), 2017. Accessed: May 14 2025. [Online]. Available: https://iopscience.iop.org/article/10.1088/1742-6596/896/1/012115

30. J. Huang, Y. Deng, P. Yi, and L. Peng, "Experimental and numerical investigation on thin sheet metal roll forming process of micro channels with high aspect ratio," The International Journal of Advanced Manufacturing Technology, vol. 100, pp. 117–129, 2019, doi: 10.1007/s00170-018-2606-5.

31. F. Reuther and M. Dix, "Virtuelle Prozesskette Der Bipolarplattenherstellung – Vom Hohlprägewalzen Bis Zum Fügen," in Fuel Cell Conference chemnitz wasserstofftechnologien. Effizient Produziert.: Chemnitzer Brennstoffzellenkonferenz Konferenzband, Nov. 2024-Nov. 2024, pp. 145–155.

32. F. Reuther, S. Melzer, A. Geist, S. Polster, and V. Psyk, "Iterativer Designprozess Für Hohlprägegewalzte Elektrolyseurplatten Am Beispiel Von „Hyventus“," in Fuel Cell Conference Chemnitz WasserstofftechnologieN. Effizient Produziert.: Chemnitzer Brennstoffzellenkonferenz Konferenzband, Nov. 2024-Nov. 2024, pp. 309–320.

33. F. Reuther, S. Winter, V. Psyk, and V. Kräusel, "Simulation of hollow embossing rolling for full-scale bipolar plates," in Material Forming, Paestum (Italy), 2025, pp. 1972–1981. Accessed: May 12 2025. [Online]. Available: https://doi.org/10.21741/9781644903599-212

34. R. Taylor, "Interpretation of the Correlation Coefficient: A Basic Review," Journal of Diagnostic Medical Sonography, vol. 6, no. 1, pp. 35–39, 1990

